Supplementary Information to Mann et al (2006) "Robustness of Proxy-Based Climate Field Reconstruction Methods" (Journal of Geophysical Research)

1. Sensitivity of NH Mean Reconstruction to Assumed Relative Error Amplitudes in Instrumental and Proxy Data

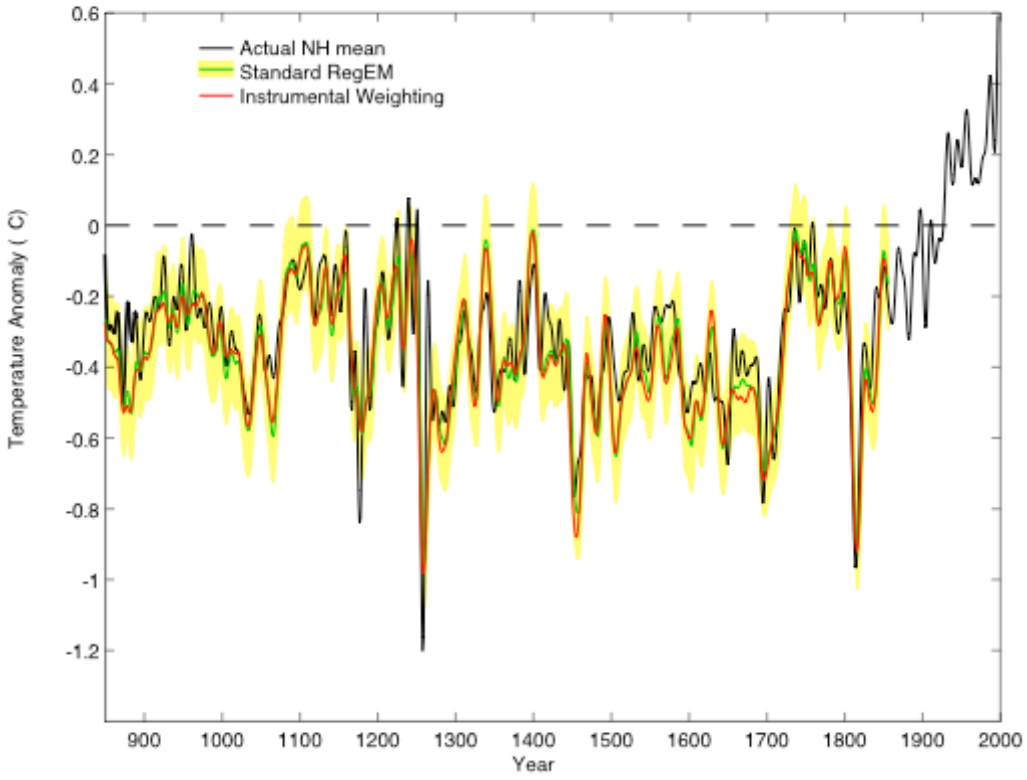

Supplementary Figure 1. Comparisons of reconstructed NH series assuming uniform relative errors (as in the main manuscript) and assuming relative error amplitudes in the proxy data that are a factor of 10 times larger than in the 'instrumental' data (this amounts to weighting the normalized instrumental data in the data matrix by a factor of 10 greater than for the 'proxy' data). Shown for comparison is the actual model NH mean series (black). The same noise realization was used in each case to facilitate assessment of the impact of the different conventions.

2. Sensitivity of NH Mean Reconstruction to Standardization Interval

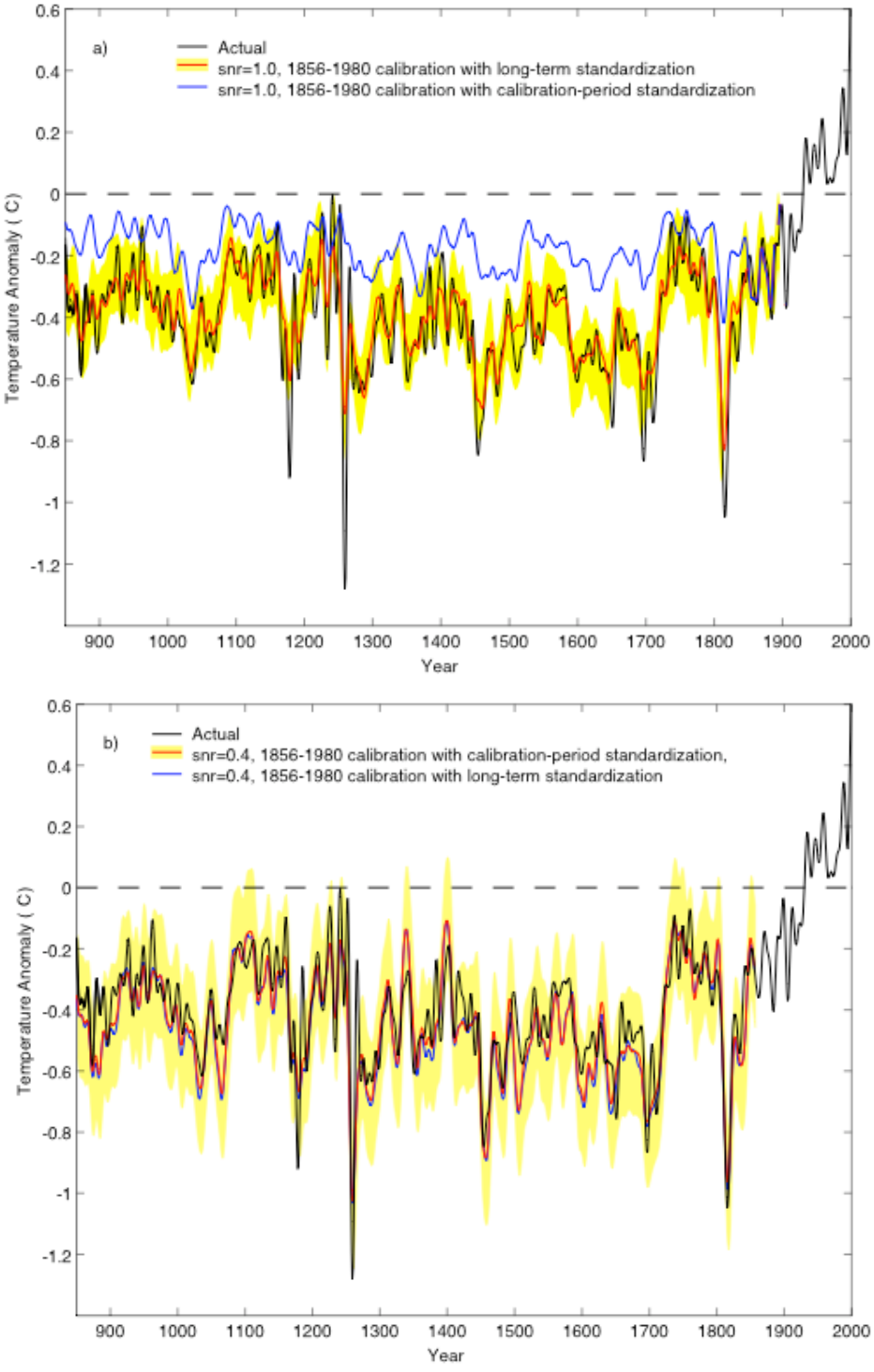

Supplementary Figure 2. Comparisons of reconstructed NH series (NCAR CSM simulation) using different standardization periods based on *(a)* RegEM with ridge regression (as used in M05) and *(b)* RegEM with TTLS (used in the present study). Shown for comparison is the actual model NH mean series (black).

3. Applications of Hybrid RegEM Method to MXD Proxy Network Used in Rutherford et al (2005)

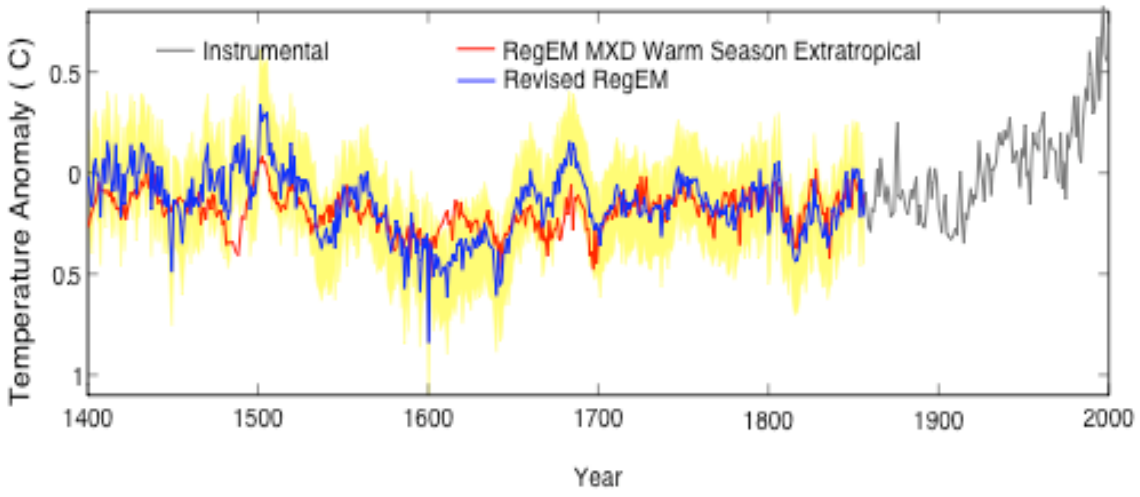

Supplementary Figure 3. Comparison between the NH warm season extratropical surface temperature reconstructions of *Rutherford et al* [2005] with the reconstruction that results from using the same (MXD) proxy datasets, but incorporating the revised version of the RegEM method discussed in the text. Series have been decadally smoothed as in main text. Shading indicated 95% confidence intervals calculated from verification residuals.

4. Impact of Incomplete Spatial Sampling (to emulate actual 19th-20th century instrumental record) on Computed NH mean Surface Temperature in CSM 1.4 Simulation

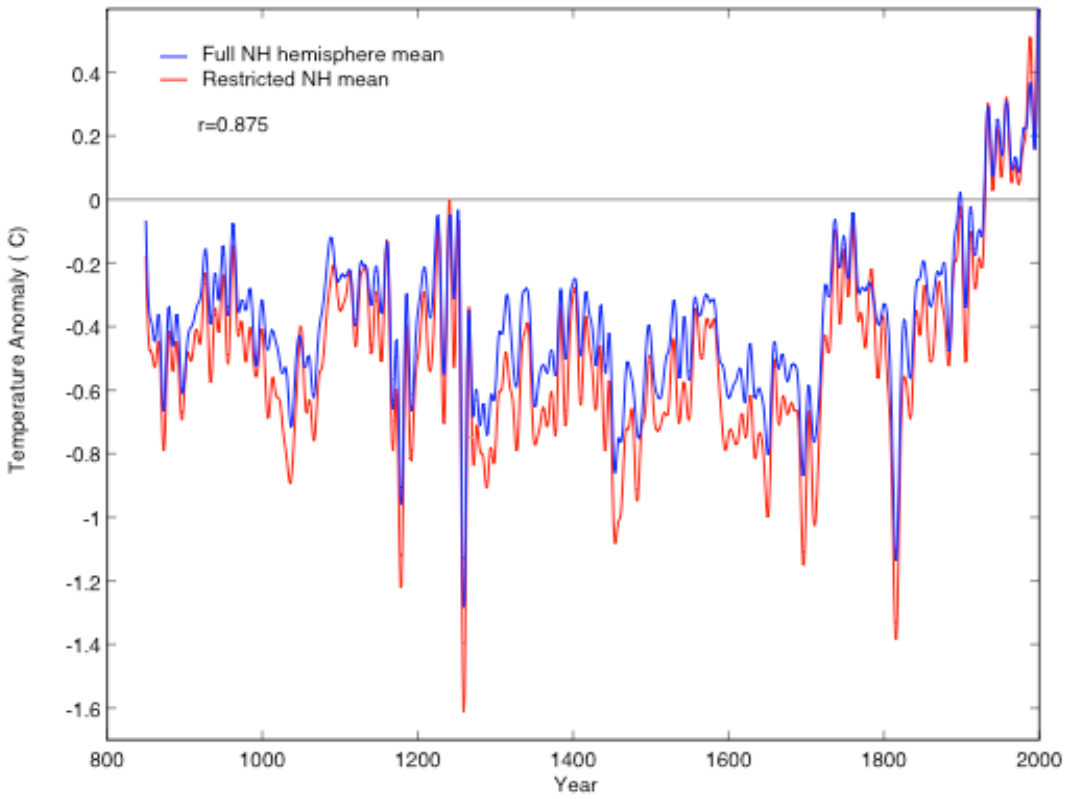

Supplementary Figure 4. Comparison of NH mean temperature anomaly series for NCAR CSM simulation resulting from use of the full model surface temperature field vs. using the restricted region of 1312 global grid box locations used in the study to simulate the actual instrumental surface temperature record.

5. Estimation of SNR for MBH and MXD proxy networks

It is most straightforward to estimate SNR in terms of the root-mean-square correlations between proxies and their associated local climate signal defined by $r = \mathrm{SNR}/(1+\mathrm{SNR}^2)^{1/2}$. For the MXD network used by R05, the gridded tree-ring data can *a priori* be considered to reflect local warm-season surface temperatures variations [see *Briffa et al*, 2001]. Estimating an appropriate value for *r* is thus relatively straightforward since the appropriate variable (surface temperature) and seasonal window (boreal warm-season) are known beforehand. We estimated (see tables below) the *r* value to range from *r=0.54* for the earliest network (26 gridded MXD series used back to AD 1400) to *r=0.48* for the full network (115 gridded MXD series available back to AD 1856).

Estimating *r* for a multiproxy dataset such as that used by MBH98 is more challenging. CFR methods do not require that a proxy indicator correlate locally with field (e.g. surface temperature) targeted for reconstruction. The signal information is assimilated not locally, but in state space through the use of both local and non-local spatial covariance information. Indeed, a primary advantage of CFR approaches to climate reconstruction is that use can be made of non-local statistical relationships between proxies and the climate field of interest. Two examples are that (i) coral and tree-ring precipitation proxies in the Western tropical Pacific or parts of Mexico are excellent predictors of eastern tropical Pacific Sea Surface Temperatures (SST) through their relationship with the El Niño-Southern Oscillation (ENSO) phenomenon, and (ii) annual accumulation measurements or oxygen isotopes from Greenland ice cores are excellent predictors of European and Eastern North American winter temperatures through their relationship with the North Atlantic Oscillation (NAO) [see e.g. section 3.2 of *Jones and Mann*, 2004]. In this case, *r* does not depend on where the proxy is located, or whether the signal information is local or non-local.

An appropriate estimate of *r* for a multiproxy network should therefore not only consider the correlation of proxy data with annual or seasonal temperatures, but also with measures of the atmospheric circulation (e.g. seasonal Sea Level Pressure) which may better be recorded by the proxy. Using this approach with the "PC/proxy" version of the MBH98 multiproxy network (wherein dense regional networks of tree-ring data were represented by their leading PCs—see R05) we estimated *r* to range from *r=0.36* for the earliest predictor network (22 indicators used back to AD 1400) to *r =0.41* for the full predictor network (112 indicators used back to AD 1820). The values are slightly lower for the "all proxy" version of the MBH98 network wherein each proxy series is represented individually (see tables below).

[Details of the calculations based on full available period of proxy/instrumental overlap intervals are provided on sheet #1 of excel spreadsheet files "MBHPCProxy, MBHAllProxy and MXD". sheets #2 and #3 of each file provide estimates over independent 'early' and 'late' sub-intervals].

I. MXD tree-ring gridbox series (data from T. Osborn of Climatic Research Unit, University of East Anglia, UK). Correlations were calculated between all MXD gridbox series and associated

instrumental temperature series (average taken over the 4 closest instrumental temperature gridboxes):

- Boreal warm-season (Apr-Sep) seasonal mean instrumental surface temperature series from 1856-1980 from Rutherford et al (2005) were used to calculate correlations
- Correlations were calculated overall, and for separate high-frequency (<20 year period) and low-frequency (>20 year period) bands:

Warm-Season Temp *r*

	Beginning Year (# available predictors)					
	1856 (115)	1800 (105)	1700 (91)	1600 (62)	1500 (40)	1400 (26)
Overall	0.49	0.49	0.49	0.48	0.49	0.54
High-Frequency	0.52	0.51	0.51	0.50	0.50	0.55
Low-Frequency	0.50	0.50	0.50	0.54	0.58	0.59

II. MBH98 multiproxy network. Correlations were calculated between indicators and both (1) local temperatures (average over the 4 nearest instrumental temperature gridboxes) and (2) local Sea Level Pressure (average over the 4 nearest instrumental SLP gridboxes) during overlapping interval

- When indicators represent PCs of spatially-distributed tree-ring networks, an approximate central geographical location for the spatial distribution was chosen based on the locations emphasized in the associated EOF pattern.
- Surface temperature gridpoint data from 1856-1980 (from Rutherford et al, 2005 as cited in paper) and SLP gridpoint data from 1871-1980 (from Zhang et al 2005 cited in paper) were used to calculate correlations.
- Temperature correlations were calculated for annual mean (Jan-Dec), boreal cold-season (Oct-Mar), and boreal warm-season (Apr-Sep) seasonal means.
- SLP correlations were calculated for boreal cold-season and warm-season means.
- Correlations were calculated overall, and for separate high-frequency (<20 year period) and low-frequency (>20 year period) bands

a. "PC/proxy" version of the MBH98 predictor network:

Highest *r* among Annual or Seasonal Temp or Seasonal SLP

	Beginning Year (# available predictors)							
	1820(112)	1800 (102)	1750 (89)	1700 (74)	1600 (57)	1500(28)	1450 (25)	1400 (22)
Overall	0.41	0.40	0.31	0.31	0.31	0.33	0.34	0.36
High-Frequency	0.41	0.39	0.29	0.29	0.29	0.31	0.30	0.32
Low-Frequency	0.62	0.62	0.62	0.59	0.59	0.60	0.61	0.62

b. "all proxy" version of the MBH98 predictor network:

Highest among Annual or Seasonal Temp or Seasonal SLP

	1820 (415)	1800 (405)	1700 (378)	1600 (317)	1500 (182)	1400 (110)
Overall	0.33	0.32	0.30	0.30	0.30	0.30
High-Frequency	0.32	0.31	0.29	0.28	0.28	0.28
Low-Frequency	0.59	0.59	0.59	0.60	0.62	0.64

6. Test of Uncertainty Estimates Using Independent Noise Realizations

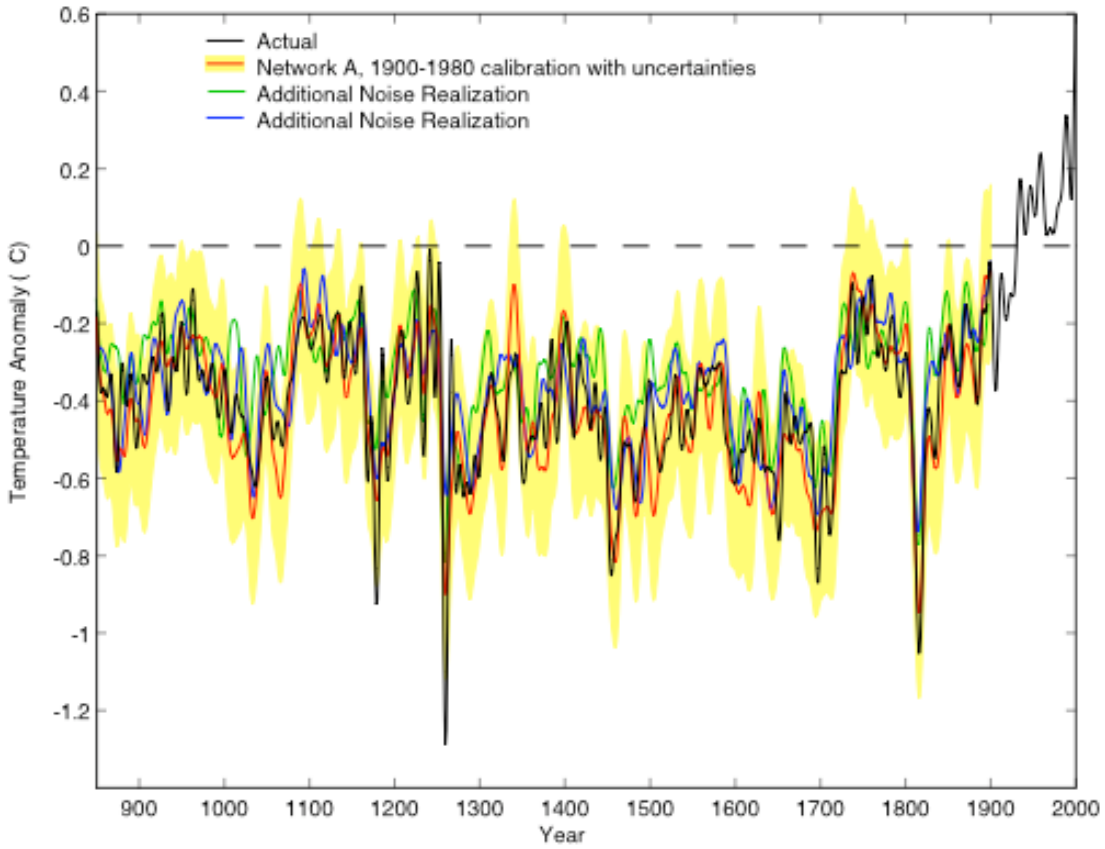

Supplementary Figure 5. Comparisons of reconstructed NH series (NCAR CSM simulation) using three different noise realizations, for Network "A" standard case SNR=0.4, white proxy noise, and 1900-1980 calibration. Shown for comparison is the actual model NH mean series (black). Long-term validation statistics for the different experiments are provided in the table below.

						NH mean			Multivariate			Niño3		
Exp.	**Net**	**SNR**	**%**	**ρ**	**Cal. Period**	**RE**	**CE**	**r^2**	**RE**	**CE**	**r^2**	**RE**	**CE**	**r^2**
a	A	0.4	86	0	1900-1980	0.95	0.67	0.71	0.36	0.04	0.10	0.80	0.11	0.53
b	A	0.4	86	0	1900-1980	0.93	0.53	0.62	0.30	-0.04	0.09	0.76	-0.08	0.27
c	A	0.4	86	0	1900-1980	0.90	0.30	0.70	0.30	-0.05	0.07	0.65	-0.31	0.19

7. Examples of AR(1) Red Noise Surrogates from Monte Carlo Simulations Used in Statistical Significance Estimation.

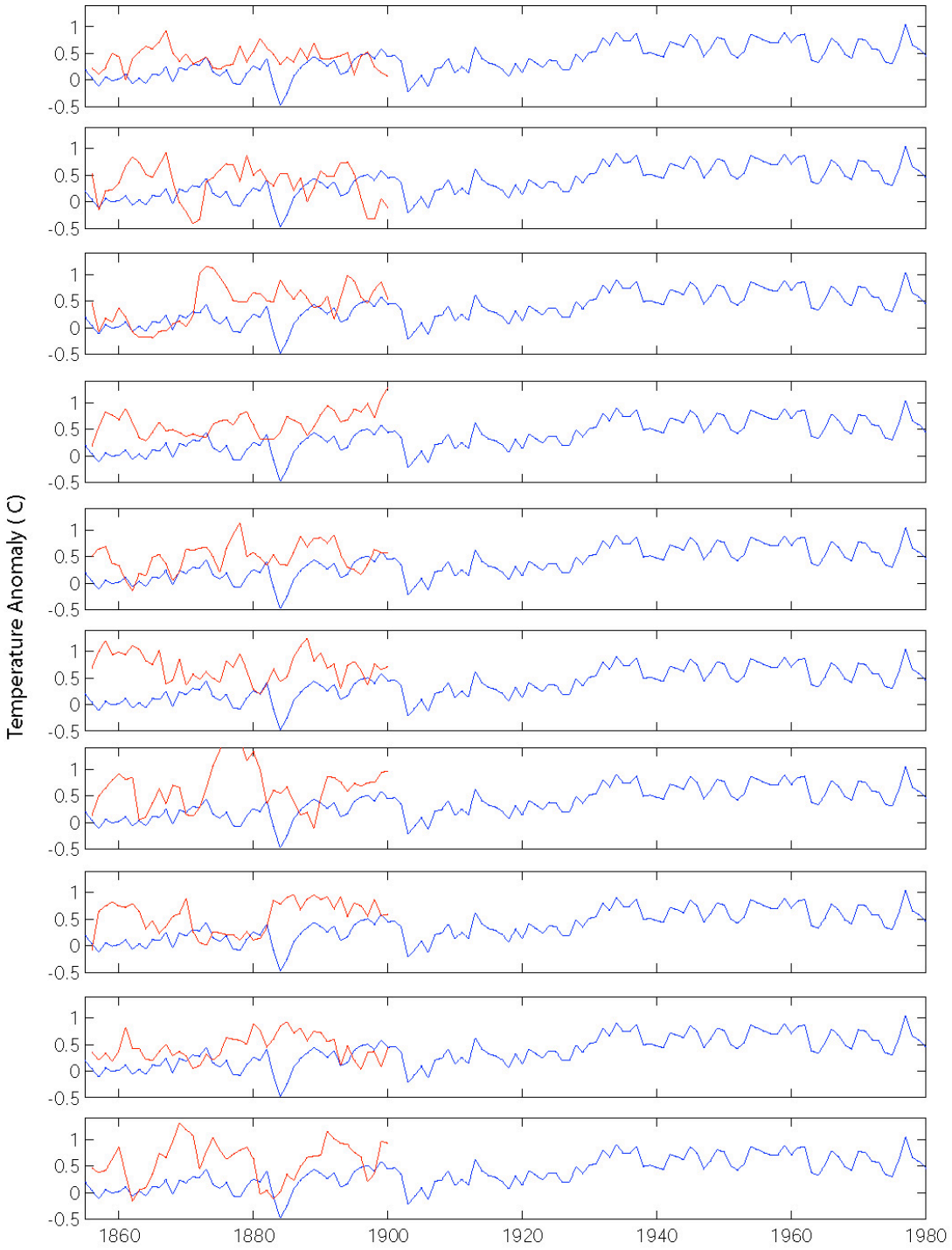

Supplementary Figure 6. Ten random AR(1) NH reconstructions (red) compared against the actual NH series using a 1900-1980 calibration and 1856-1899 validation period. Note the general failure of the (stationary) AR(1) surrogates to capture the systematic (non-stationary) decrease in the mean over the validation interval.

8. Details of Application of Objection Selection Criteria to the Experiments Described in the Main Text

Exp.	Net	SNR	%	ρ	Cal. Period	*M*	*K high*	*K low*
a	A	∞	0	0	1856-1980	6	5	1
b	A	∞	0	0	1900-1980	5	5	1
	A	∞	0	0	1900-1980[1]	5	5	1
c	D	∞	0	0	1856-1980	6	5	1
d	A	∞	0	0	1856-1980	6	5	1
e	A	1.0	50	0	1856-1980	6	5	2
f	A	0.5	80	0	1856-1980	4	4	2
g	A	0.4	86	0	1856-1980	4	4	3
h	A	0.25	94	0	1856-1980	2	2	3
i	A	0.4	86	0	1900-1980	3	4	2
	A	0.4	86	0	1900-1980[1]	3	4	2
j	B	0.4	86	0	1900-1980	1	1	1
	B	0.4	86	0	1900-1980[1]	1	1	1
k	C	0.4	86	0	1900-1980	1	1	1
	C	0.4	86	0	1900-1980[1]	1	1	1
l	A	0.4	86	0	1856-1980	4	4	3
m	A	0.4	86	0	1900-1980	3	4	2
	A	0.4	86	0	1900-1980[1]	3	4	2
n	D	0.4	86	0	1856-1980	4	6	3
o	D	0.4	86	0	1900-1980	4	4	2
	D	0.4	86	0	1900-1980[1]	4	4	2
p	A	1.0	50	0.32	1856-1980	6	5	1
q	A	1.0	50	0.32	1900-1980	5	5	2
	A	1.0	50	0.32	1900-1980[1]	5	5	2
r	A	0.4	86	0.32	1856-1980	3	6	3
s	A	0.4	86	0.32	1900-1980	3	3	2
	A	0.4	86	0.32	1900-1980[1]	3	3	2
t (GK)	A	1.0	50	0.32	1856-1980	3	3	1
u (GK)	A	1.0	50	0.32	1900-1980	2	3	1
	A	1.0	50	0.32	1900-1980[1]	2	3	1
v (GK)	A	0.4	86	0.32	1856-1980	2	2	3
w (GK)	A	0.4	86	0.32	1900-1980	2	2	2
	A	0.4	86	0.32	1900-1980[1]	2	2	2
x	A	0.4	86	0	1900-1980D	3	3	2
	A	0.4	86	0	1900-1980D[1]	3	3	2
y (GK)	A	0.4	86	0	1900-1980	2	2	2
	A	0.4	86	0	1900-1980[1]	2	2	2
z (GK)	A	0.4	86	0	1900-1980D	2	2	2
	A	0.4	86	0	1900-1980D[1]	2	2	2

Supplementary Table 1. TTLS truncation parameters *K_high* and *K_low* and number of instrumental PCs *M* used in each of the experiments in the main text

9. Nino3 Reconstructions.

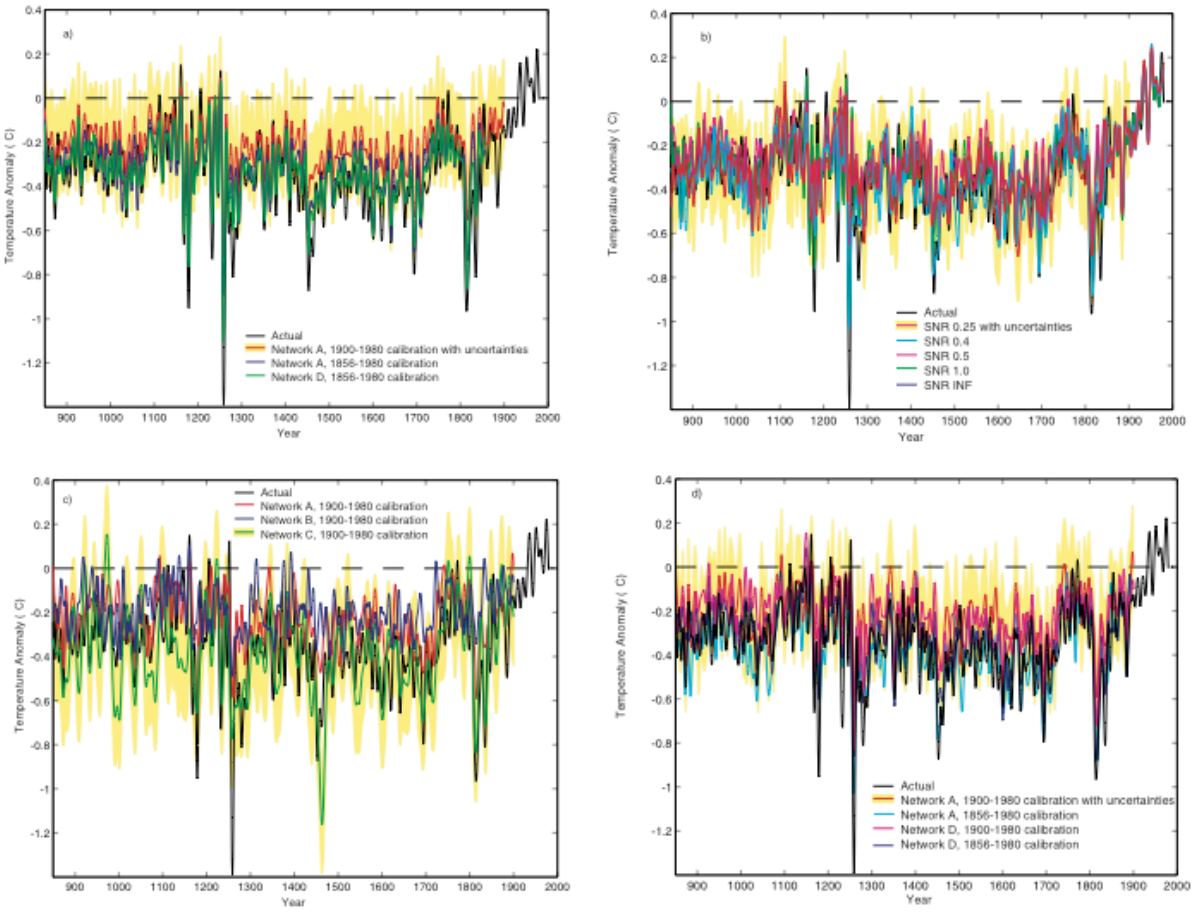

Supplementary Figure 7. Same as Figure 3 in manuscript, but comparing reconstructed and actual Niño3 series rather than NH mean series (NCAR CSM simulation).

10. Test of Red Proxy Noise Using "Sparse" Pseudoproxy Grid C.

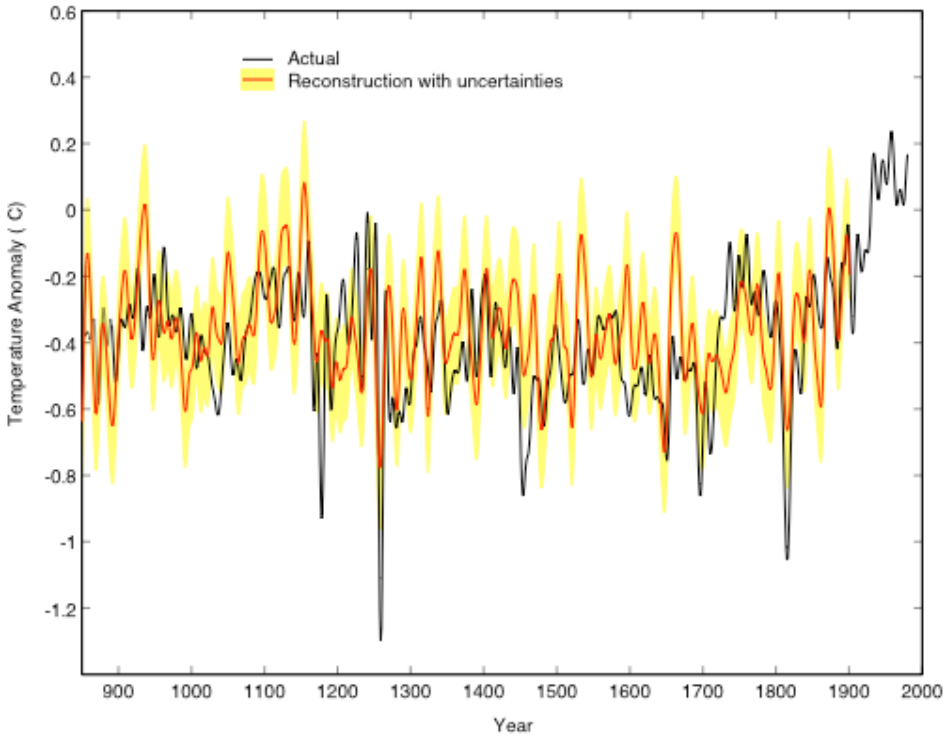

Supplementary Figure 8. Comparisons of reconstructed NH series using "sprase" pseudoproxy network "C", NCAR CSM short (1900-1980) calibration, SNR=0.4, and "red" proxy noise with ρ=0.32. Both short and long-term validation statistics are provided in the table below.

						NH mean			Multivariate			Niño3		
Exp.	**Net**	**SNR**	**%**	**ρ**	**Cal. Period**	**RE**	**CE**	**r^2**	**RE**	**CE**	**r^2**	**RE**	**CE**	**r^2**
a	C	0.4	86	0.32	1900-1980	0.85	-0.09	0.18	0.25	-0.12	0.03	0.77	-0.04	0.12
b	C	0.4	86	0.32	1900-1980'	0.73	-0.91	0.56	0.12	-0.17	0.06	0.58	-0.19	0.31

11. Test of Sensitivity of RegEM NH mean reconstruction to varying levels of noise autocorrelation.

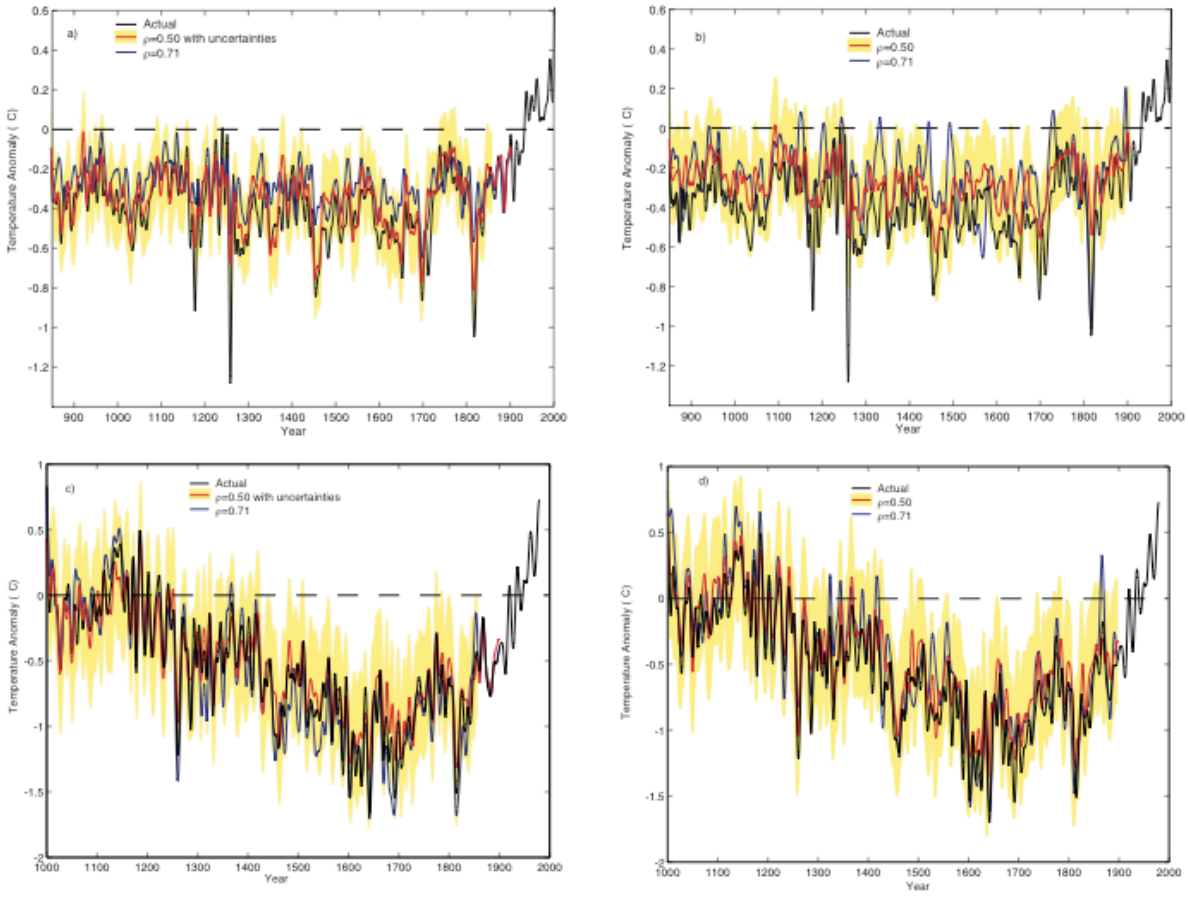

Supplementary Figure 9. Comparisons of reconstructed NH series using pseudoproxy network "A", SNR=0.4, and "red" proxy noise with noise autocorrelation levels of both ρ=0.5 and ρ=0.71. Results are shown for: *a)* NCAR CSM long (1856-1980) calibration, *b)* NCAR CSM short (1900-1980) calibration, *c)* GKSS "Erik" long (1856-1980) calibration, *d)* GKSS "Erik" short (1900-1980) calibration. The same noise realization was used for both in each of the experiments. Long-term validation statistics are provided in the table below.

						NH mean			Multivariate			Niño3		
Exp.	**Net**	**SNR**	**%**	**ρ**	**Cal. Period**	**RE**	**CE**	**r^2**	**RE**	**CE**	**r^2**	**RE**	**CE**	**r^2**
a	A	0.4	86	0.5	1856-1980	0.92	0.59	0.65	0.30	-0.04	0.03	0.73	0.11	0.31
b	A	0.4	86	0.5	1900-1980	0.87	0.07	0.64	-0.04	-0.35	0.04	0.71	-0.20	0.20
c	A	0.4	86	0.71	1856-1980	0.77	-0.12	0.48	0.25	0.02	0.11	0.61	0.07	0.24
d	A	0.4	86	0.71	1900-1980	0.79	-0.51	0.29	0.25	-0.12	0.07	0.48	-0.44	0.12
e GK	A	0.4	86	0.5	1856-1980	0.96	0.88	0.91	0.66	0.43	0.51	0.83	0.65	0.79
f GK	A	0.4	86	0.5	1900-1980	0.93	0.81	0.89	0.62	0.35	0.43	0.80	0.60	0.71
g GK	A	0.4	86	0.71	1856-1980	0.94	0.85	0.90	0.68	0.45	0.55	0.82	0.75	0.81
h GK	A	0.4	86	0.71	1900-1980	0.91	0.77	0.86	0.63	0.37	0.43	0.83	0.71	0.79

12. Additional Sensitivity Experiments Discussed in Section 4.6 of Text.

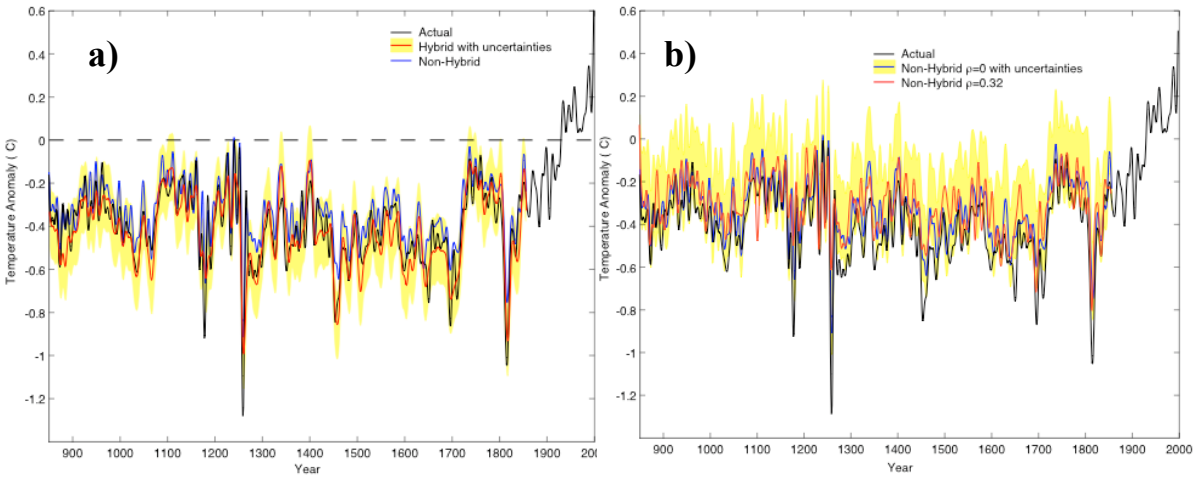

Supplementary Figure 10. Comparison of reconstructed NH series (NCAR CSM simulation) using non-hybrid and hybrid (as in main text) version of RegEM routine, for (a) Network "A", SNR=0.4, and long (1856-1980) calibration and (b) Comparing non-hybrid reconstruction for white and red proxy noise cases. Long-term validation statistics are provided in the table below.

						NH mean			Multivariate			Niño3		
Exp.	Net	SNR	%	ρ	Cal. Period	RE	CE	r^2	RE	CE	r^2	RE	CE	r^2
a	hyb	0.4	86	0	1856-1980	0.95	0.67	0.74	0.37	0.07	0.18	0.90	0.26	0.55
b	no-hyb	0.4	86	0	1856-1980	0.90	0.50	0.59	0.25	0.03	0.09	0.83	0.04	0.51

						NH mean			Multivariate			Niño3		
Exp.	Net	SNR	%	ρ	Cal. Period	RE	CE	r^2	RE	CE	r^2	RE	CE	r^2
a	A	0.4	86	0.32	1856-1980	0.83	0.16	0.63	0.32	0.12	0.17	0.58	-0.09	0.27
b	A	0.4	86	0	1856-1980	0.90	0.50	0.59	0.25	0.03	0.09	0.83	0.04	0.51

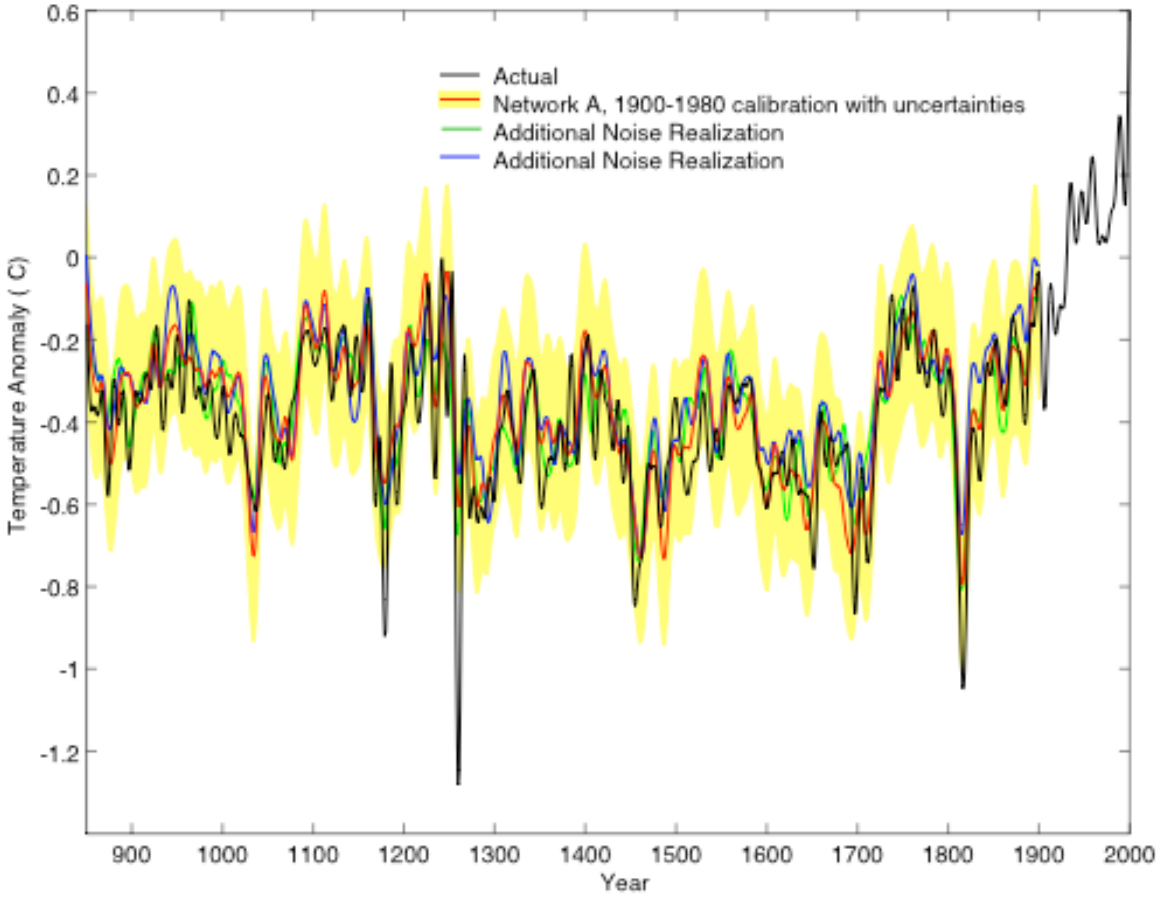

Supplementary Figure 11. Comparisons of reconstructed NH series (NCAR CSM simulation) for network "A" SNR=0.4, white proxy noise, and short (1900-1980) calibration, where the actual SNR value for individual pseudoproxies is allowed to vary randomly over the range 0.1 to 0.7 while preserving the ensemble mean value SNR=0.4. Results are shown for three different realizations. Shown for comparison is the actual model NH mean series (black). Long-term validation statistics are provided in the table below.

						NH mean			Multivariate			Niño3		
Exp.	**Net**	**SNR**	**%**	**ρ**	**Cal. Period**	**RE**	**CE**	**r^2**	**RE**	**CE**	**r^2**	**RE**	**CE**	**r^2**
a	A	var	var	0	1900-1980	0.92	0.42	0.61	0.35	0.04	0.12	0.64	-0.21	0.17
b	A	var	var	0	1900-1980	0.94	0.58	0.65	0.31	-0.03	0.11	0.73	-0.06	0.34
c	A	var	var	0	1900-1980	0.94	0.61	0.69	0.35	0.03	0.12	0.80	0.07	0.35

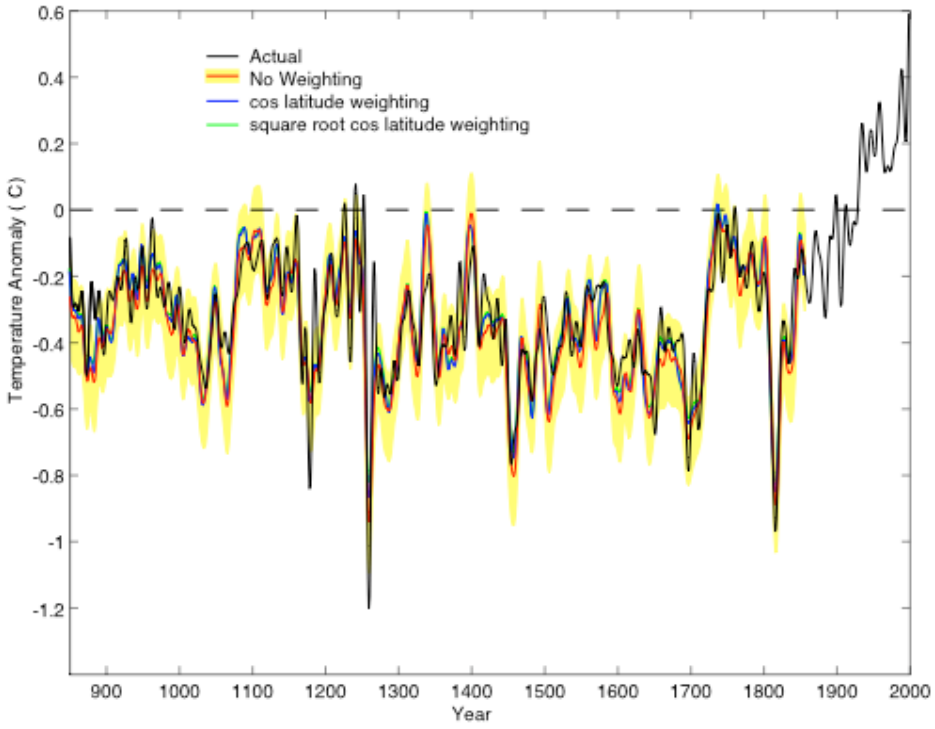

Supplementary Figure 12. Comparisons of reconstructed NH series (NCAR CSM simulation) using two different surface temperature areal weighting schemes (both amplitude and variance-based gridbox areal weighting schemes) and no areal weighting, for Network "A" standard case SNR=0.4, white proxy noise, and long (1856-1980) calibration. Shown for comparison is the actual model NH mean series (black). The same noise realization was used in each case. Long-term validation statistics are provided in the table below.

						NH mean			Multivariate			Niño3		
Exp.	**Net**	**SNR**	**%**	**ρ**	**Cal. Period**	**RE**	**CE**	**r^2**	**RE**	**CE**	**r^2**	**RE**	**CE**	**r^2**
a	A	0.4	86	0	1856-1980	0.95	0.67	0.74	0.37	0.07	0.18	0.90	0.26	0.55
lat	A	0.4	86	0	1856-1980	0.94	0.71	0.74	0.33	0.13	0.18	0.76	0.18	0.31
sqrt	A	0.4	86	0	1856-1980	0.94	0.71	0.73	0.32	0.11	0.17	0.74	0.17	0.27

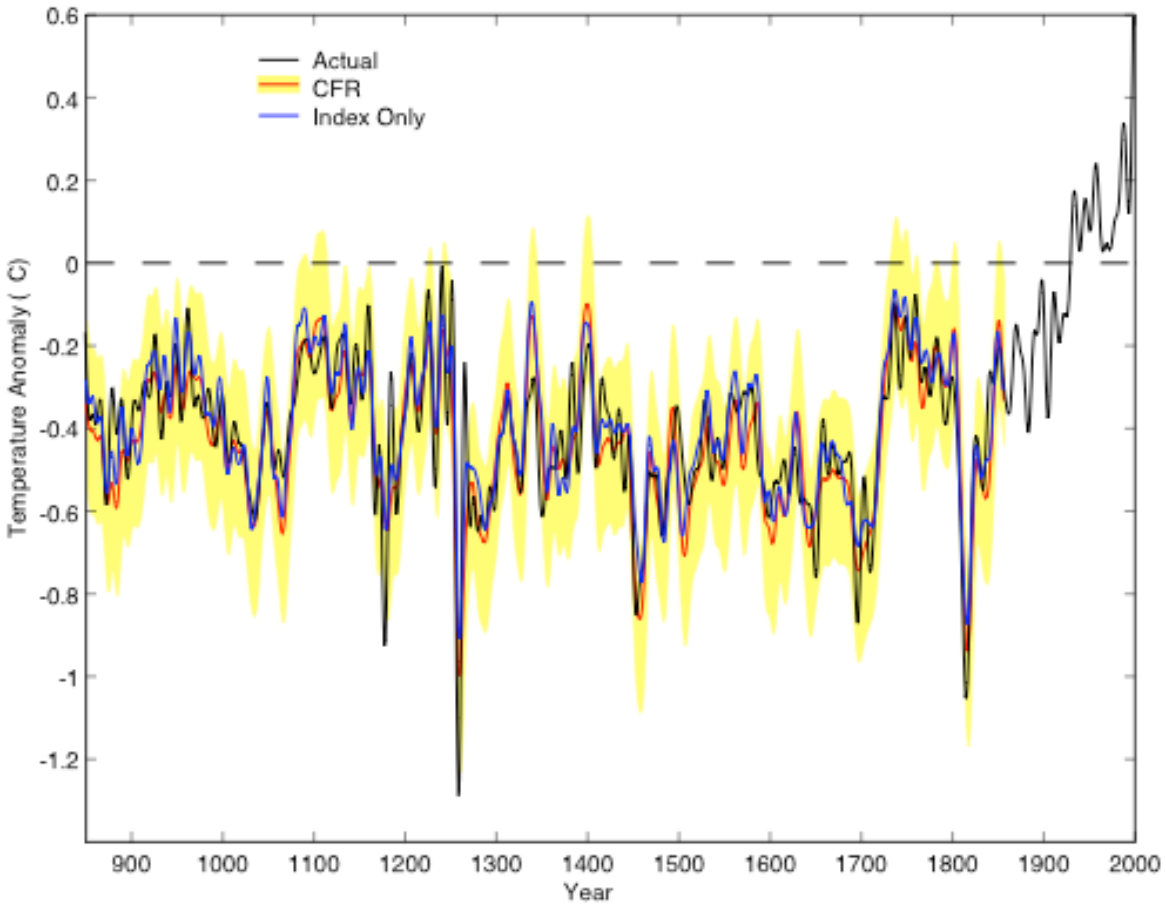

Supplementary Figure 13. Comparisons of reconstructed NH series (NCAR CSM simulation) using "index only" and "full field" surface temperature reconstruction approach, for Network "A", SNR=0.4, white proxy noise, and long (1856-1980) calibration. Shown for comparison is the actual model NH mean series (black). The same noise realization was used in both cases. Long-term validation statistics are provided in the table below.

						NH mean			Multivariate			Niño3		
Exp.	**Net**	**SNR**	**%**	**ρ**	**Cal. Period**	**RE**	**CE**	**r^2**	**RE**	**CE**	**r^2**	**RE**	**CE**	**r^2**
g	A	0.4	86	0	1856-1980	0.95	0.67	0.74	0.37	0.07	0.18	0.90	0.26	0.55
b	A	0.4	86	0	1856-1980	0.96	0.74	0.75	N/A	N/A	N/A	N/A	N/A	N/A

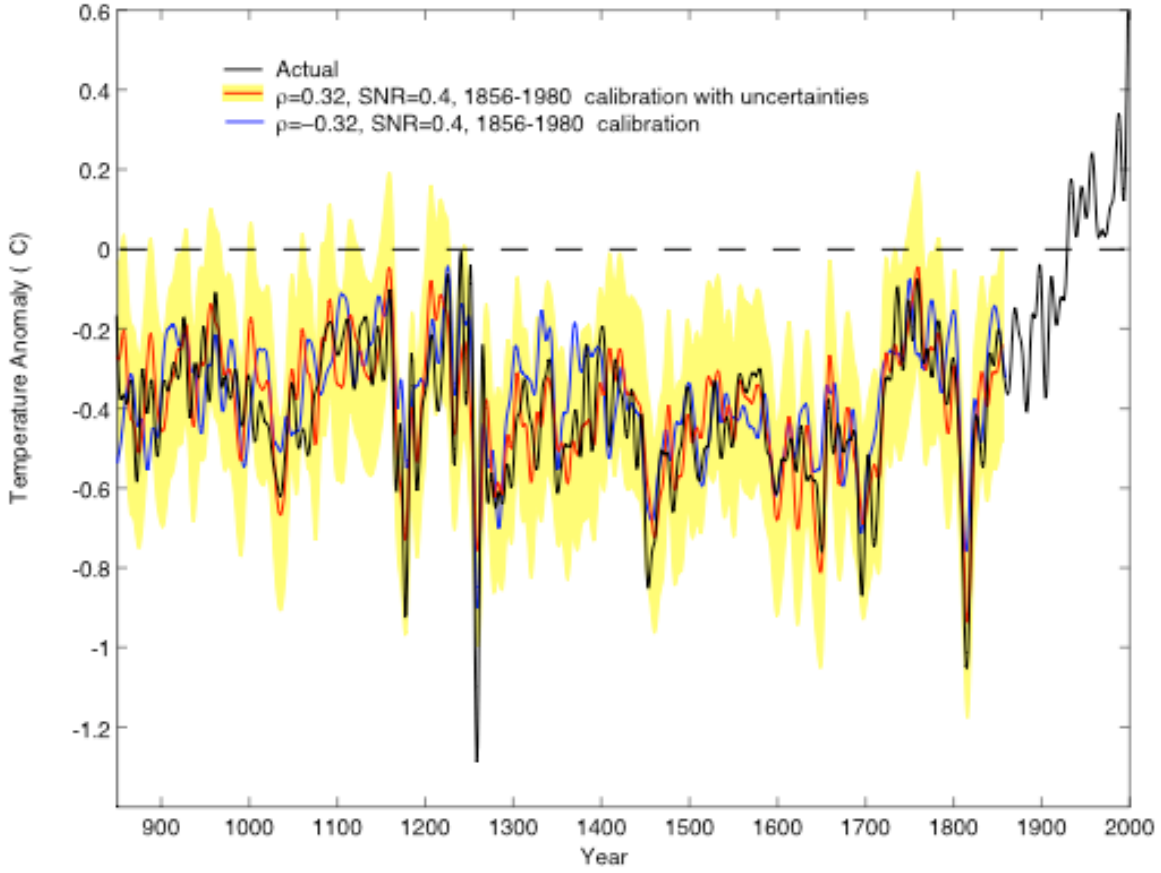

Supplementary Figure 14. Comparisons of reconstructed NH series (NCAR CSM simulation) using both "red" proxy noise with ρ=0.32 and "blue" proxy noise ρ=-0.32, for Network "A" SNR=0.4, and 1856-1980 calibration. Shown for comparison is the actual model NH mean series (black). The same noise realization was used in each case. Long-term validation statistics are provided in the table below.

						NH mean			Multivariate			Niño3		
Exp.	**Net**	**SNR**	**%**	**ρ**	**Cal. Period**	**RE**	**CE**	**r^2**	**RE**	**CE**	**r^2**	**RE**	**CE**	**r^2**
a	A	0.4	86	0.32	1856-1980	0.94	0.63	0.66	0.31	-0.03	0.15	0.86	0.01	0.45
b	A	0.4	86	-0.32	1900-1980	0.90	0.52	0.60	0.22	-0.01	0.11	0.86	0.10	0.55

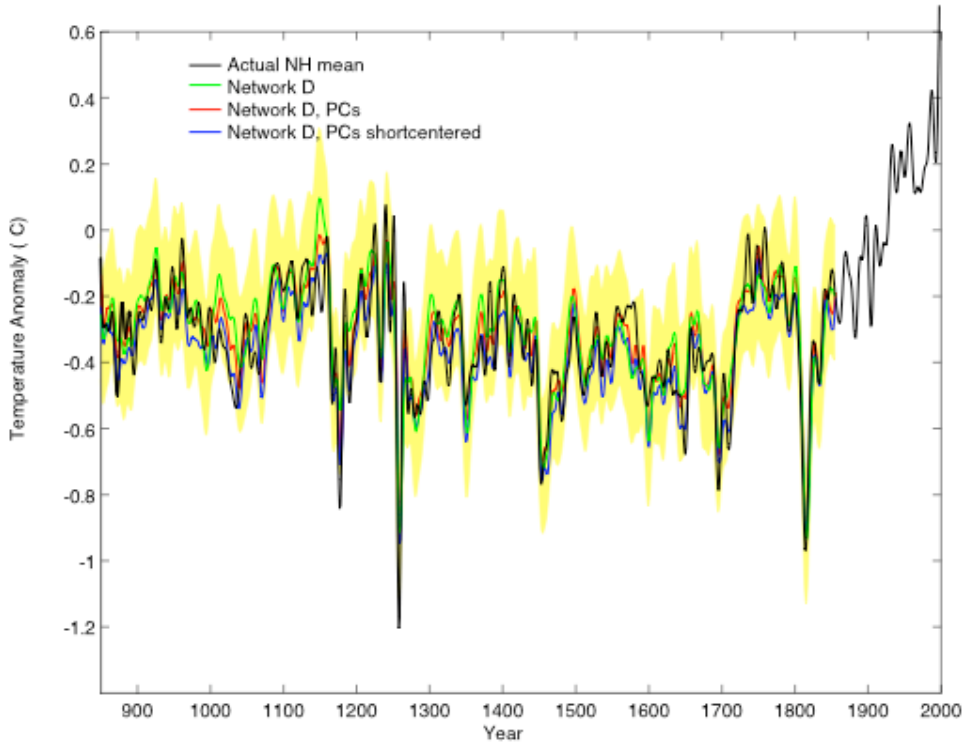

Supplementary Figure 15. Comparisons of reconstructed NH series (NCAR CSM simulation) using all (208) individual pseudoproxy series of Network "D" and PC summary representations of pseudoproxy data set using the leading statistically significant PC series as determined by the procedure described in manuscript. Results are shown using both (long-term and calibration period only) PCA standardization conventions discussed in text. Comparisons are for SNR=0.4, white proxy noise, and long (1856-1980) calibration. Shown for comparison is the actual model NH mean series (black). Long-term validation statistics are provided in the table below**.**

						NH mean			Multivariate			Niño3		
Exp.	**Net**	**SNR**	**%**	**ρ**	**Cal. Period**	**RE**	**CE**	**r^2**	**RE**	**CE**	**r^2**	**RE**	**CE**	**r^2**
pcshort	D	0.4	86	0	1856-1980	0.95	0.78	0.83	0.17	-0.08	0.05	0.71	0.11	0.64
pc	D	0.4	86	0	1856-1980	0.96	0.81	0.82	0.19	-0.05	0.06	0.84	0.30	0.68
n	D	0.4	86	0	1856-1980	0.95	0.66	0.69	0.40	0.15	0.21	0.92	0.45	0.71

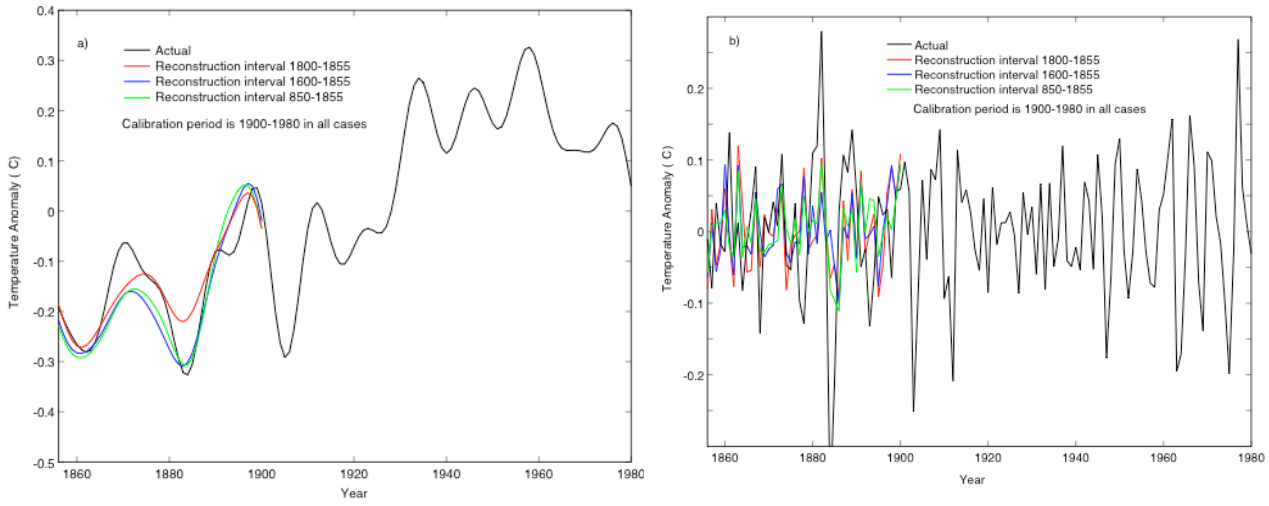

Supplementary Figure 16. Influence of length of reconstruction interval on NH reconstruction for both (a) low-frequency and (b) high-frequency component of hybrid reconstruction method based NCAR CSM short (1900-1980) calibration using pseudoproxy network "A", SNR=0.4, and white proxy noise.

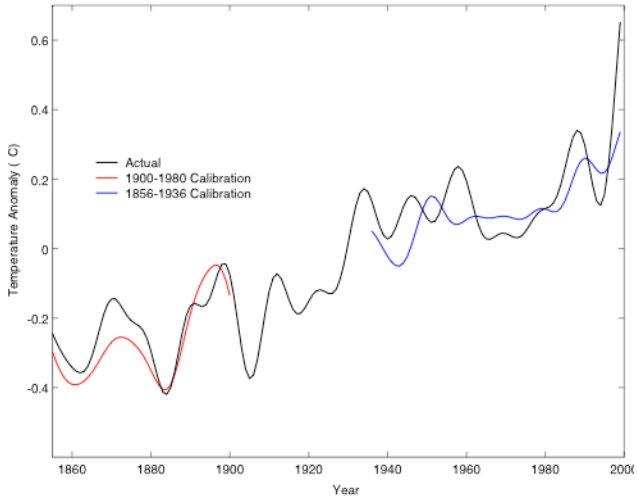

Supplementary Figure 17. Comparison of standard 'early' validation results for two different 'late' validation experiments based on NH reconstructions using two different alternative 'early' calibration periods. Results are based on CSM 1.4, Network "A", and SNR=0.4. Low-frequency component of reconstruction is shown. The same noise realization (corresponding to experiment "i" in the paper) is used in all cases (SNR=0.4, ρ=0). The noise realization was extended to 1999 for these experiments. Validation statistics are provided in the table below.

						NH mean		
Exp.	Net	SNR	%	ρ	Cal. Period	RE	CE	r^2
a	A	0.4	86	0	1856-1936	0.94	0.44	0.47
b	A	0.4	86	0	1900-1980	0.95	0.66	0.82

13. Additional Experiments Testing Effect of Detrending Data over Calibration Interval.

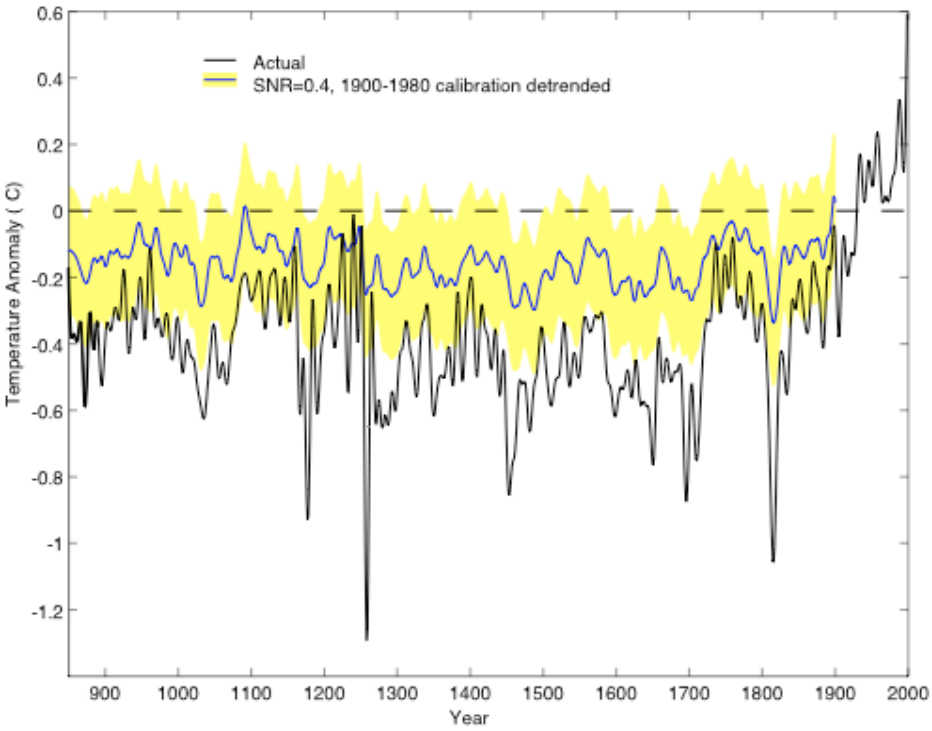

Supplementary Figure 18. Reconstructed NH series as in Figure 6 of manuscript, but based on detrending both predictors (pseudoproxies) and predictand (surface temperature field) over calibration interval. Reconstructions are based on NCAR CSM short (1900-1980) calibration using pseudoproxy network "A", SNR=0.4, and white proxy noise.

14. Spatial Pattern of *RE* Statistic

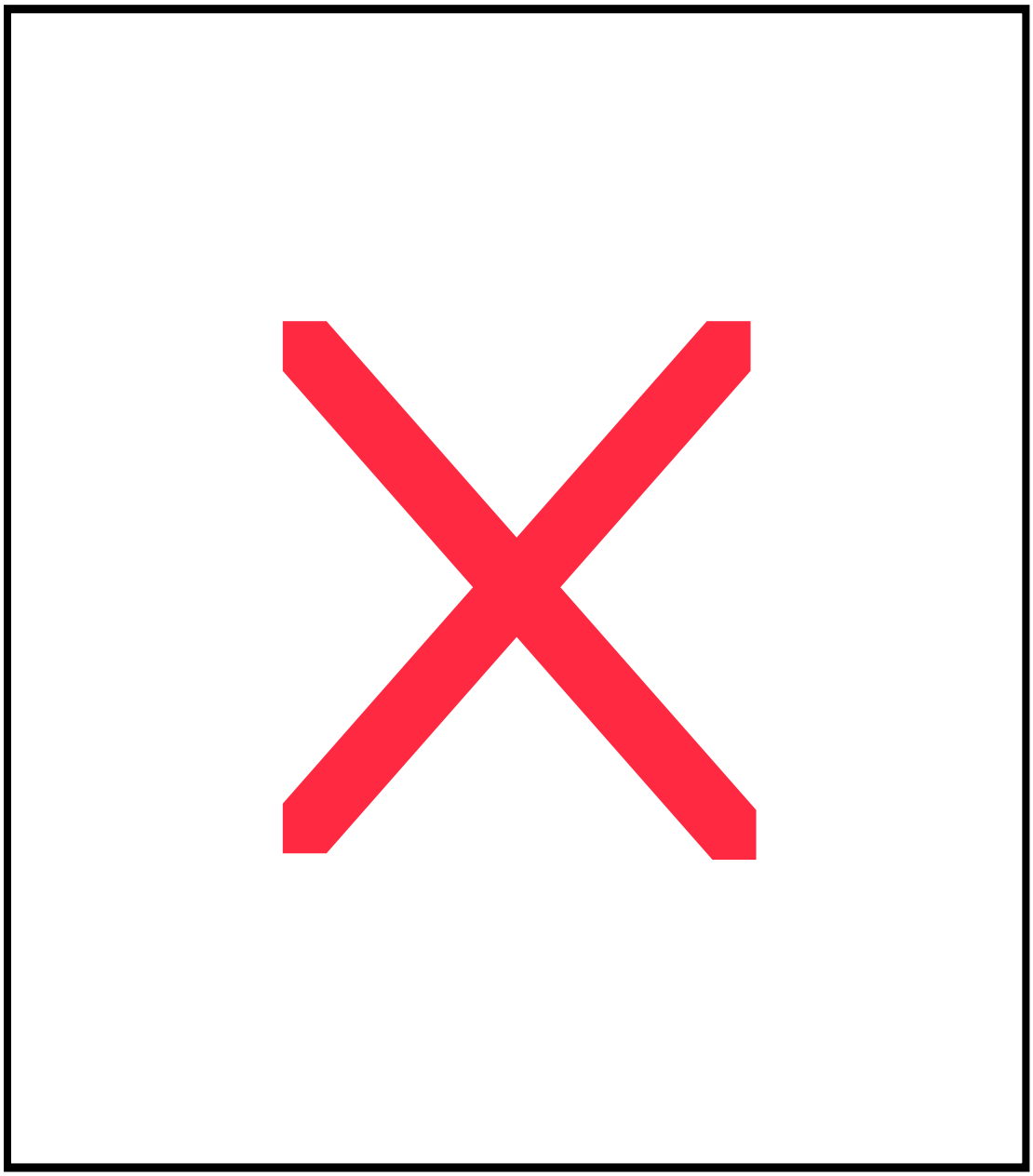

Supplementary Figure 19. ‘Gridbox *RE* long-term (850-1855) verification scores corresponding to reconstructions shown in Figure 6 of the paper

15. Multivariate ('mult') Statistics Using Global Temperature Field

						Full Multivariate		
Exp.	**Net**	**SNR**	**%**	**ρ**	**Cal. Period**	**RE**	**CE**	**r^2**
a	A	∞	0	0	1856-1980	0.37	0.17	0.21
b	A	∞	0	0	1900-1980	0.30	-0.06	0.17
	A	∞	0	0	1900-1980[1]	0.23	-0.03	0.14
c	D	∞	0	0	1856-1980	0.30	0.07	0.23
d	A	∞	0	0	1856-1980	0.37	0.17	0.21
e	A	1.0	50	0	1856-1980	0.33	0.12	0.17
f	A	0.5	80	0	1856-1980	0.33	0.12	0.15
g	A	0.4	86	0	1856-1980	0.23	-0.02	0.12
h	A	0.25	94	0	1856-1980	0.20	-0.05	0.06
i	A	0.4	86	0	1900-1980	0.30	-0.06	0.12
	A	0.4	86	0	1900-1980[1]	0.21	-0.06	0.11
j	B	0.4	86	0	1900-1980	0.26	-0.11	0.04
	B	0.4	86	0	1900-1980[1]	0.13	-0.16	0.03
k	C	0.4	86	0	1900-1980	0.23	-0.16	0.05
	C	0.4	86	0	1900-1980[1]	0.12	-0.17	0.04
l	A	0.4	86	0	1856-1980	0.23	-0.02	0.12
m	A	0.4	86	0	1900-1980	0.30	-0.06	0.12
	A	0.4	86	0	1900-1980[1]	0.21	-0.06	0.11
n	D	0.4	86	0	1856-1980	0.40	0.09	0.20
o	D	0.4	86	0	1900-1980	0.31	-0.04	0.16
	D	0.4	86	0	1900-1980[1]	0.20	-0.06	0.14
p	A	1.0	50	0.32	1856-1980	0.32	0.11	0.17
q	A	1.0	50	0.32	1900-1980	0.26	0.03	0.14
	A	1.0	50	0.32	1900-1980[1]	0.24	-0.01	0.14
r	A	0.4	86	0.32	1856-1980	0.14	-0.14	0.12
s	A	0.4	86	0.32	1900-1980	0.27	-0.10	0.12
	A	0.4	86	0.32	1900-1980[1]	0.21	-0.05	0.09
t (GK)	A	1.0	50	0.32	1856-1980	0.70	0.53	0.58
u (GK)	A	1.0	50	0.32	1900-1980	0.61	0.39	0.51
	A	1.0	50	0.32	1900-1980[1]	0.56	0.18	0.31
v (GK)	A	0.4	86	0.32	1856-1980	0.64	0.44	0.50
w (GK)	A	0.4	86	0.32	1900-1980	0.55	0.30	0.39
	A	0.4	86	0.32	1900-1980[1]	0.48	0.03	0.16
x	A	0.4	86	0	1900-1980D	0.14	-0.31	0.04
	A	0.4	86	0	1900-1980D[1]	0.00	-0.33	0.05
y (GK)	A	0.4	86	0	1900-1980	0.63	0.42	0.50
	A	0.4	86	0	1900-1980[1]	0.57	0.20	0.37
z (GK)	A	0.4	86	0	1900-1980D	0.02	-0.54	0.22
	A	0.4	86	0	1900-1980D[1]	0.06	-0.75	0.27

Supplementary Table 2. 'mult' validation statistics using global (Southern Hemisphere as well as Northern Hemisphere) gridboxes as shown in Figure 2 of the manuscript.

16. Frequency-dependence of signal-to-noise ratio for pseudoproxy networks.

Raw SNR	ρ	low-f corr.	high-f corr.	raw corr.
Network A				
0.25	0	0.35	0.22	0.24
0.4	0	0.52	0.35	0.37
0.5	0	0.61	0.42	0.45
1.0	0	0.84	0.67	0.71
0.4	0.32	0.43	0.36	0.37
1.0	0.32	0.74	0.69	0.71
Network B				
0.4	0	0.47	0.34	0.36
Network C				
0.4	0	0.48	0.33	0.35
GKSS				
0.4	0	0.66	0.29	0.37
0.4	0.32	0.55	0.30	0.37
1.0	0.32	0.84	0.62	0.71

Supplementary Table 3. Average correlations for the various pseudoproxy networks used, overall and restricted to low-frequency and high-frequency bands used in analysis.